The American Journal of Pathology, Vol. 187, No. 6, June 2017

ELSEVIER

The American Journal of PATHOLOGY

ajp.amjpathol.org

VASCULAR BIOLOGY, ATHEROSCLEROSIS, AND ENDOTHELIUM BIOLOGY

Interferon-γ Released by Activated CD8$^+$ T Lymphocytes Impairs the Calcium Resorption Potential of Osteoclasts in Calcified Human Aortic Valves

Edit Nagy,*†‡ Yang Lei,* Eduardo Martínez-Martínez,* Simon C. Body,§¶ Florian Schlotter,* Michael Creager,* Alexander Assmann,*‖ Kamal Khabbaz,** Peter Libby,* Göran K. Hansson,† and Elena Aikawa*

From the Division of Cardiovascular Medicine, Department of Medicine, Brigham and Women's Hospital, Harvard Medical School, Boston, Massachusetts; the Department of Medicine,† Karolinska Institute, Stockholm, Sweden; the Department of Cardiology,‡ Karolinska University Hospital, Stockholm, Sweden; the Center for Perioperative Genomics§ and Department of Anesthesiology,¶ Brigham and Women's Hospital, Boston, Massachusetts; the Department of Cardiovascular Surgery,‖ Heinrich Heine University Medical School, Duesseldorf, Germany; and the Division of Cardiac Surgery,** Department of Surgery, Beth Israel Deaconess Medical Center, Boston, Massachusetts

Accepted for publication February 9, 2017.

Address correspondence to Elena Aikawa, M.D., Ph.D., Division of Cardiovascular Medicine, Department of Medicine, Brigham and Women's Hospital, Harvard Medical School, 77 Ave Louis Pasteur, NRB-741, Boston, MA 02115. E-mail: eaikawa@partners.org.

In calcific aortic valve disease (CAVD), activated T lymphocytes localize with osteoclast regions; however, the functional consequences of this association remain unknown. We hypothesized that CD8$^+$ T cells modulate calcification in CAVD. CAVD valves ($n = 52$) dissected into noncalcified and calcified portions were subjected to mRNA extraction, real-time quantitative PCR, enzyme-linked immunosorbent assay, and immunohistochemical analyses. Compared with noncalcified portions, calcified regions exhibited elevated transcripts for CD8, interferon (IFN)-γ, CXCL9, Perforin 1, Granzyme B, and heat shock protein 60. Osteoclast-associated receptor activator of NK-κB ligand (RANKL), tartrate-resistant acid phosphatase (TRAP), and osteoclast-associated receptor increased significantly. The stimulation of tissue with phorbol-12-myristate-13-acetate and ionomycin, recapitulating CAVD microenvironment, resulted in IFN-γ release. Real-time quantitative PCR detected mRNAs for CD8$^+$ T-cell activation (Perforin 1, Granzyme B). In stimulated versus unstimulated organoid cultures, elevated IFN-γ reduced the mRNAs encoding for RANKL, TRAP, and Cathepsin K. Molecular imaging showed increased calcium signal intensity in stimulated versus unstimulated parts. CD14$^+$ monocytes treated either with recombinant human IFN-γ or with conditioned media-derived IFN-γ exhibited low levels of Cathepsin K, TRAP, RANK, and tumor necrosis factor receptor-associated factor 6 mRNAs, whereas concentrations of the T-cell co-activators CD80 and CD86 increased in parallel with reduced osteoclast resorptive function, effects abrogated by neutralizing anti–IFN-γ antibodies. CD8$^+$ cell–derived IFN-γ suppresses osteoclast function and may thus favor calcification in CAVD. *(Am J Pathol 2017, 187: 1413–1425; http://dx.doi.org/10.1016/j.ajpath.2017.02.012)*

Nonrheumatic aortic valve stenosis remains the leading valvulopathy. Its increasing prevalence in the aged population renders the disease the most common indication for either surgical or percutaneous valve implantation.[1,2] Although established cardiovascular risk factors, such as hyperlipidemia, age, smoking, obesity, diabetes mellitus, hypertension, sex, and renal failure contribute to the development both of calcific aortic valve stenosis and atherosclerosis,[3] the therapeutic response to statin treatment differs substantially between these two diseases, because statins do not consistently retard the progression of aortic valve stenosis.[4] Histologic studies of aortic valves show that inflammation precedes extracellular matrix remodeling,[5] which along with lipid deposition, neovascularization, and

Supported by the Swedish Research Council grant 537-2013-484, the Swedish Heart-Lung Foundation (E.N.), German Heart Foundation grant S/04/12 (A.A.), and NIH grants R01HL114823 (S.C.B.), R01HL114805 (E.A.), and R01HL109506 (E.A.).

Disclosures: None declared.

http://dx.doi.org/10.1016/j.ajpath.2017.02.012

ectopic mineralization leads to fibrocalcific disease progression.[6–8] Pronounced calcification of the valve characterizes this disease[1] and correlates with the stenosis severity and independently predicts outcome.[9] Affected aortic valves contain numerous activated T lymphocytes[6] that express the IL-2 receptor.[10] T-cell receptor repertoire analysis identifies these cells as predominantly clonally expanded memory-effector $CD8^+$ T cells that display evidence of activation.[11,12] The peripheral blood of patients with aortic valve stenosis also harbors these cells.[12] The presence of shared T-cell clones between tissue and peripheral blood suggests lymphocyte trafficking from the circulation into valvular tissue.[12] Furthermore, the blood of patients with calcific aortic valve disease (CAVD) shows more $CD8^+$ versus $CD4^+$ T cells than unaffected individuals, as well as an expanded $CD4^+$ $CD28^-$ T-cell population, the latter mostly in patients with concomitant atherosclerotic disease.[12] This observation contrasts with the composition of atheroma, which contain a polyclonal lymphocyte population.[13,14]

Moreover, in calcific aortic valve tissue, both the leukocytes surrounding calcium deposits and approximately 30% of the valvular interstitial cells localized in the fibrosa and spongiosa layers,[15] which display human leukocyte antigen (HLA)—antigen-D related (DR), a major histocompatibility complex (MHC) class II protein. These results indicate that similar to atherosclerotic lesions,[16] activated T cells in stenotic valves secrete interferon (IFN)-γ,[17] a major inducer of class II MHC expression,[17] which is also expressed by vascular smooth muscle cells[18] and valvular interstitial cells.[15] Collectively, these observations point to the participation of adaptive immunity in CAVD.

IFN-γ, the signature T helper 1 cytokine, activates macrophages[19] and promotes atherosclerosis by increasing the antigen-presenting capacity of macrophages, inducing the expression of numerous key chemokines and chemokine receptors, facilitates expression of adhesion molecules by endothelial cells, and induces expression of genes regulating lipid transport.[16] In addition, previous studies show that CAVD tissue contains increased transcripts that encode heat shock protein (Hsp) 60[8] and immunoreactive oxidized low-density lipoprotein,[20] two established candidate autoantigens in atherosclerosis that closely correlate with T-cell infiltrates, calcium deposits,[20] and neoangiogenesis.[8]

Overall, these studies suggest that an adaptive immune response operates in CAVD through the activation of circulating $CD8^+$ cells, their clonal expansion and differentiation to the memory-effector subtype, and exchanges of these T-cell clones between the peripheral blood and valve.[12] In addition, IFN-γ production by $CD8^+CD28^-$ T cells may drive ectopic calcification.[12] The functional implication of activated effector T lymphocytes and their cytokine release in the affected valvular tissue may impair osteoclast function, thus increasing valvular calcium accumulation. Previous observations described the presence of osteoclasts in CAVD,[21,22] yet their functional state and osteoresorptive potential remains largely unknown. Activated T cells participate pivotally in inflammatory bone disease, leading to bone resorption and high turnover osteopenia.[23] In contrast, terminally differentiated activated $CD8^+$ T cells strongly suppress osteoclastogenesis.[24,25] However, the simultaneously highly expressed receptor activator of nuclear factor-κB ligand (RANKL), released by activated T cells and osteoblasts, compromises the inhibitory effect of IFN-γ and may lead to the formation of functional osteoclasts, albeit with reduced resorptive potential.[26]

We hypothesized that excessive valve calcification arises in part from compromised osteoclasts function due to IFN-γ released by activated T cells. Although many publications have reported that valvular interstitial cells can differentiate into functional osteoblast-like cells, few, if any, have assessed the role of osteoclasts in CAVD. Therefore, we focused on the assessment of valvular osteoclasts in end-stage CAVD. We examined the functional role of activated IFN-γ—secreting $CD8^+$ T cells residing in calcific aortic valve tissue and their association with valvular calcium content. The results support a causal relation between the presence of activated valvular IFN-γ—secreting $CD8^+$ T cells and increased calcification, which contributes to the progression of stenosis in human CAVD.

Materials and Methods

Patients

Explanted calcified aortic valves were obtained from 52 patients (38 men and 14 women; mean age, 69.8 ± 10 years) undergoing elective aortic valve replacement surgery without history of rheumatic valve disease, infective endocarditis, recent immunosuppressive therapy, or human immunodeficiency virus or hepatitis C seropositivity. Five patients had bicuspid aortic valves. Patients with prosthetic valve deterioration requiring repeat surgery were excluded from the study cohort. Of the included patients, 44% had concomitant obstructive coronary artery disease and underwent coronary artery bypass grafting surgery concurrently with valve replacement, except for one patient who had elective coronary artery bypass grafting 6 months before aortic valve replacement.

Table 1 shows patient characteristics. The study was approved by Brigham and Women's Hospital Institutional Review Board protocols (2010P002567; 2011P001703). All patients gave written informed consent.

Echocardiography

All included patients underwent two-dimensional transthoracic Doppler echocardiographic imaging studies according to the standard recommendations of the

Table 1 Patient Characteristics

Characteristic	Explanted aortic valves
Patients	52
Male sex	38 (73)
Age, years	70 (45–87)
AVA, cm^2	0.8 (0.4–1.1)
AVA/BSA, cm^2/m^2	0.38 (0.2–0.63)
P-max, mmHg	76 (42–125)
P-mean, mmHg	47 (22–69)
LVEF, %	60 (30–79)
LVEDD, mm	45 (35–68)
Comorbidities	
Diabetes mellitus	13 (25)
Presence of obstructive coronary artery disease	23 (44.2)
Hyperlipidemia	38 (73)
Hypertension	40 (76.9)
Renal dysfunction	4 (7.7)
Serum creatinine, μmol/L	84.86 (47.73–646.2)
Smoker status	
Current	1 (1.92)
No smoker	28 (53.8)
Former	23 (44.2)
HbA1c, %	5.75 (4.8–12)
Medication	
Acetylsalicylic acid	36 (69.2)
Angiotensin receptor blockade	10 (19.2)
ACE inhibitor	19 (36.5)
β-Blocker	26 (50)
Statin	37 (71.1)
Ca-antagonist	11 (21.1)

Values are n (%) or median (range).

ACE, angiotensin-converting enzyme; AVA, aortic valve area; AVA/BSA, aortic valve area, indexed for body surface area; LVEF, left ventricle ejection fraction; HbA1c, glycated hemoglobin; LVEDD, left ventricular end-diastolic diameter; P-max, maximal transvalvular pressure; P-mean, mean transvalvular pressure.

European Association of Echocardiography and American Society of Echocardiography[27] (Philips IE33 system; Philips Medical Systems, Andover, MA) at Brigham and Women's Hospital. The quantification of aortic valve stenosis was based on the aortic valve area (in cm^2), the aortic valve area indexed for body surface area (in cm^2/m^2), and the calculated maximum and mean transvalvular pressure gradients, (in mmHg). The left ventricular dimensions and function were within normal range in all of the included patients except for one patient who had concomitant moderate-to-severe aortic valve regurgitation with a left ventricular ejection fraction of 30% (Table 1).

Macroscopic Dissection and Sample Preparation

Aortic valve leaflets were divided into noncalcified and calcified portions based on gross morphologic characteristics. The samples were stored in RNA Later solution (76104; Qiagen, Caldwell, NJ) to preserve RNA. Total RNA from 100 mg of homogenized valve tissue (116 samples from 46 explanted aortic valves; six additional valves were used for immunohistochemistry) was extracted using the RNeasy Lipid Tissue Mini kit (74804; Qiagen) and subjected to first-strand cDNA synthesis from 0.5 μg of RNA according to the manufacturer's instructions (High-capacity cDNA Reverse Transcription Kit, 4368814; Applied Biosystems, Foster City, CA) after measuring the RNA concentration spectrophotometrically at 260 nm (A260/280 nm; NanoDrop 2000/2000c; Thermo Fisher Scientific Inc., Waltham, MA). In addition, one piece of each valve specimen was incubated for 24 hours in serum-free Dulbecco's modified Eagle's medium and embedded into OCT-compound for histologic analysis.

TaqMan Real-Time PCR

Quantitative TaqMan PCR was performed on a 7900HT Fast Real-Time PCR system (Applied Biosystems) with the following primers/probes from Applied Biosystems: glyceraldehyde-3-phosphate dehydrogenase, Hs02786624_g1; IFN-γ, Hs00989291_m1; IFN-γ receptor 1, Hs00988304_m1; monokine induced by IFN-γ (CXCL9), Hs00171065_m1; class II MHC transactivator (CIITA), Hs00172094_m1; CD8A, Hs00233520_m1; CD4, Hs01058407_m1; Perforin 1, Hs00169473_m1; Granzyme B (GZMB), Hs01554355_m1; RANKL [tumor necrosis factor superfamily 11 (TNFSF11)], Hs00243522_m1; forkhead box P3, Hs01085834_m1; tartrate-resistant acid phosphatase (TRAP; ACP5), Hs00356261_m1; Cathepsin K, Hs00166156_m1; CXCL10, Hs01124251_g1; CXCL11, Hs04187682_g1; and CCL2 (monocyte chemoattractant protein 1), Hs00234140_m1. Primers/probes for osteoclast-associated receptor (OSCAR; Hs01100185) was from Thermo Fisher Scientific Inc. For real-time quantitative PCR analyses of the $CD14^+$ cells, the following primers/probes (Applied Biosystems) were used: RANK (TNFRSF11A), Hs00921372_m1; TNF receptor-associated factor 6 (TRAF6), Hs00371512_g1; CD80, Hs00175478_m1; and CD86, Hs01567026_m1. The reactions contained 5 μL of TaqMan Fast Universal PCR Master Mix (4352042; Applied Biosystems). mRNA levels were normalized for the expression levels of glyceraldehyde-3-phosphate dehydrogenase, which served as a reference message.

Unstimulated Organoid Cultures

Surgically explanted human aortic valve specimens were transported on ice in cell culture medium from the operating room and dissected into noncalcified and calcified regions. One portion of the tissues was incubated for 24 hours at 37°C in serum-free Dulbecco's modified Eagle's medium containing 50 IU/mL penicillin, 100 IU/mL streptomycin, and 2.5 μg/mL amphotericin B. The concentrations of IFN-γ and RANKL were measured using enzyme immunoassay kits [Human IFN-γ ELISA (enzyme-linked immunosorbent assay) Kit EHIFNG2; Thermo Scientific and Human

TNFSF11/RANKL PicoKine ELISA Kit EK0842; Booster, Pleasanton, CA], according to the manufacturer's instructions. The concentrations were normalized for the protein content measured in each conditioned medium (Pierce BCA Protein assay kit 23227; Thermo Fisher Scientific Inc.).

Organoid Cultures Stimulated with Polyclonal Activators

The second portion of the explanted leaflet was incubated overnight in serum-free α-minimal essential medium (M 2279; Sigma-Aldrich, St. Louis, MO) containing antibiotics (50 IU/mL penicillin, 100 IU/mL streptomycin, and 2.5 μg/mL amphotericin B) in the presence of phorbol-12-myristate 13-acetate (PMA) and ionomycin (Cell Activation Cocktail without Brefeldin A: premixed cocktail with optimized concentration of PMA and ionomycin; 423301/100 μL; BioLegend, San Diego, CA) to activate the T lymphocytes residing in the valve tissue. Before starting the stimulation, a sample of each conditioned medium was kept at −20°C for later analysis to obtain the baseline concentrations of IFN-γ and RANKL.

For stimulation, the manufacturer's recommendation of 2 μL of cell activation cocktail to each milliliter of the cell culture supernatant fluids was followed and added to the cell culture medium containing the minced valve tissue as recommended for activation of isolated T cells. By the end of each 24 hours of stimulation, the media were collected at 37°C, centrifuged, filtered through a 0.22-μm filter (MILLEX GV; Merck Millipore Ltd., Kenilworth, NJ), and stored at −20°C. The concentrations of IFN-γ were determined by enzyme immunoassay (Human IFN-γ ELISA Kit EHIFNG2; Thermo Fisher Scientific Inc.). Measurements of RANKL concentration used an ELISA kit (Human TNFSF11/RANKL PicoKine ELISA Kit EK0842; Booster).

After an overnight stimulation and measurement of IFN-γ concentrations, the cell-free conditioned medium [diluted to a final concentration of 0.5 ng/mL and supplemented with 10% heat-inactivated fetal bovine serum (FBS)] was used to stimulate $CD14^+$ cells in the presence or absence of a neutralizing anti−IFN-γ antibody (eBioscience 16-7318; Affymetrix, San Diego, CA) at 10 μg/mL, a concentration 1000 times in excess of that required for neutralization of the IFN-γ activity.

After the first 24 hours of stimulation, the medium was harvested by centrifugation, sterilely filtrated, stored at −20°C, and labeled as After/1. The medium to the minced valvular tissue was then replenished and supplemented with an equivalent amount of cell activation cocktail for a further 24 hours of stimulation, labeled as After/2. By the end of 2 days of stimulation, the medium and the minced valvular tissue were collected, and the latter one was stored in RNA Later (76104; Qiagen) at −80°C for mRNA extraction.

Molecular Imaging of Mineralization of Unstimulated and Stimulated Calcified Organoid Culture Systems and Quantification of Time-Lapse Images

In a subset of explanted calcified valve specimens ($n = 4$), the stimulation protocol was prolonged up to day 3 after a previous 24 hours of incubation (5 nmol/L) with a near infrared fluorescence calcium tracer (OsteoSense750 EX, NEV10053EX; PerkinElmer, Waltham, MA), which binds to nanocrystals of hydroxyapatite and elaborates fluorescence detectable through the near infrared window (excitation/emission: 750/780 nm), as previously described.[28] From each calcified valve tissue, two pieces were cut and used for the unstimulated and stimulated experiments, whereby cell activation cocktail was added into the conditioned medium at every 24 hours.

To counterbalance the decreasing fluorescent signal intensity over time in the tissue, the conditioned medium of the unstimulated and the stimulated parts was supplemented with 1 nmol/L OsteoSense750 EX every 24 hours. In parallel with sequential imaging every 24 hours, the conditioned medium was collected and stored at −20°C for analysis of IFN-γ and RANKL concentrations. Images were taken by Kodak ImageStation 4000M Pro (Kodak, Rochester, NY). For subsequent quantitative imaging analyses, at first, the GNU image program (GIMP 2.8) was used to align the time-series of images. Fluorescence signal intensity measurements were performed within a particular region of interest on each image, and the distribution of signal intensity was demonstrated on Image Histograms, an operation mode converting two-dimensional spatial information and therefore used to characterize its content, defined by a region of interest. All subsequent image analyses were performed using ImageJ software version 1.49k (NIH, Bethesda, MD; *http://imagej.nih.gov/ij*).

Immunofluorescence and Immunohistochemical Staining

Transversal cryosections (6 μm) oriented from the cusp base to the free edge were fixed in acetone and subjected to immunofluorescence staining using monoclonal mouse anti-human CD8 (dilution 1:50; M 7103; Dako, Glostrup, Denmark) and polyclonal rabbit anti-human IFN-γ antibody (dilution 1:200; ab9657; Abcam, Cambridge, UK). For immunohistochemical analysis the following antibodies were used: polyclonal rabbit anti-human CXCL9 (dilution 1:50; NBP1-31155; Novus Biologicals, Littleton, CO), monoclonal mouse anti-human Perforin 1 (dilution 1:25; ab47225; Abcam), polyclonal rabbit anti-human GZMB (dilution 1:25; ab4059; Abcam), monoclonal mouse anti-human TRAP (ready-to-use; PA0093; Novocastra Leica, Nussloch, Germany), polyclonal rabbit anti-human Cathepsin K (dilution 1:100; ab19027; Abcam), polyclonal rabbit anti-human Hsp60 antibody (dilution 1:200; NBP1-04303; Novus Biologicals), monoclonal mouse

anti-human HLA-DR antibody (dilution 1:200; M 0746; Dako, Santa Clara, CA), monoclonal mouse anti-human RANKL (dilution 1:25; NBP100-56512; Novus Biologicals), and polyclonal rabbit anti-human OSCAR (dilution 1:100; ab93817; Abcam). Cells were quantified in five high-power fields for each calcified and noncalcified regions in five donors.

$CD14^+$ Cell Isolation from Peripheral Blood of Healthy Individuals

$CD14^+$ monocytes were isolated from the buffy coat from six healthy individuals using Dynabeads FlowComp Human CD14 immunomagnetic positive selection Kit (11367D; Invitrogen, Carlsbad, CA) according to the manufacturer's instructions, as described previously.[29] Briefly, 30 mL of buffy coat (Research Blood Components) were separated by lymphocyte separation medium (0850494X-100 mL; MP Biomedicals, Santa Ana, CA), washed by Hanks' balanced salt solution (45001-152; Corning Cellgro, Manassas, VA), specifically purified by CD14 antibody and yielded 30 to 60 million $CD14^+$ monocytes. These isolated $CD14^+$ monocytes were maintained in α-minimal essential medium (M 2279; Sigma-Aldrich) supplemented with 10% heat-inactivated FBS (Life Technologies, Carlsbad, CA); 1% L-glutamine, penicillin, and streptomycin (Sigma-Aldrich); and cultured on 6-well plates (2×10^6 cells/well) for mRNA isolation, Corning Osteo Assay Surface 24-well plates for bone resorption analysis (0.5×10^6 cells/well; Corning Life Sciences, Corning, NY), and 96-well plates for TRAP staining and immunofluorescence. After 4 days of maintenance of the isolated monocytes in differentiation medium, which contained 25 ng/mL recombinant human macrophage colony-stimulating factor (M-CSF) and 30 ng/mL human recombinant RANKL (310-01; PeproTech, Rocky Hill, NJ), the following treatments were used: i) recombinant human M-CSF alone with a concentration of 25 ng/mL, served as a negative control; ii) M-CSF (25 ng/mL) + soluble RANKL (30 ng/mL); iii) M-CSF + RANKL + recombinant human IFN-γ (rh IFN-γ) (0.5 ng/mL; 285-IF; R&D Systems, McKinley, MN); iv) M-CSF + RANKL + rh IFN-γ (0.5 ng/mL) + Anti-human IFN-γ Functional Grade Purified (10 μg/mL; 16-7318; Affymetrix eBioscience); v) M-CSF + RANKL + natural IFN-γ from conditioned medium (diluted to a final concentration of 0.5 ng/mL and supplemented with 10% heat-inactivated FBS); vi) M-CSF + RANKL + natural IFN-γ from conditioned medium (diluted to a final concentration of 0.5 ng/mL and supplemented with 10% heat-inactivated FBS) + Anti-human IFN-γ Functional Grade Purified (10 μg/mL); and vii) in the last treatment condition, the osteoclast precursors were treated with M-CSF + RANKL + rh IFN-γ (0.5 ng/mL) + and a normal rabbit IgG antibody (sc-2027; Santa Cruz Biotechnology, Dallas, TX), without neutralizing the IFN-γ effect (data not shown). In three treatment conditions (iv, vi, and vii), the cell culture supernatant fluids containing either rh IFN-γ or natural IFN-γ were incubated with Anti-human IFN-γ Functional Grade Purified for 1 hour at room temperature before being added to the cell cultures. Half the cell culture medium with the cytokines was changed twice a week, and cells were maintained for 14 days.

TRAP Staining and Quantification

TRAP staining and quantification were performed using the TRAP staining kit (PMC-AK04F-COS; B-Bridge International, Santa Clara, CA). Briefly, cells on 96-well plates were washed by phosphate-buffered saline, fixed by 10% formalin for 5 minutes at room temperature, and stained by chromogenic substrate for up to 60 minutes. $TRAP^+$ cells with three or more nuclei were considered as osteoclasts and counted in triplicate wells. For detection of actin ring, cells were fixed and permeabilized with 0.1% Triton X-100 (9002-93-1; Sigma-Aldrich) and incubated with Rhodamine Phalloidin (dilution 1:40; R415; Life Technologies, Carlsbad, CA). Images were captured with a fluorescence confocal microscope (Nikon Eclipse 80i; Nikon, Tokyo, Japan).

Resorption Pit Assay for Functional Osteoclast Analysis

On day 14, cells were removed with 10% bleach for 10 minutes at room temperature. The wells were washed twice with distilled water and dried for 3 to 5 hours at room temperature. Afterward, resorption pit images were taken using a light microscope. Images were converted to black and white binary images for quantification of pit area using ImageJ.

Statistical Analysis

Clinical parameters, gene expression, and ELISA data are expressed as medians and ranges. After Shapiro-Wilk normality test and equality variance test, single comparisons were analyzed by *U*-test for gene expression parameters and ELISA measurements. For statistical analyses for comparison of multiple groups, one-way analysis of variance and for all pairwise multiple comparisons Dunn's method was used. $P < 0.05$ was considered significant. Analyses were performed with SigmaPlot software version 11 (Systat Software, Inc., San Jose, CA).

Results

Expression Profile of $CD8^+$ T Cells and Osteoclasts in Human CAVD

The calcified regions of the explanted aortic valve tissue exhibited transcriptional profiles with significantly elevated markers for IFN-γ–producing $CD8^+$ T cells (CD8A mRNA: 2.8- ± 0.6-fold, $P = 0.028$; IFN-γ mRNA: 4.35- ± 2.1-fold, $P = 0.007$) (Figure 1, A and B, and

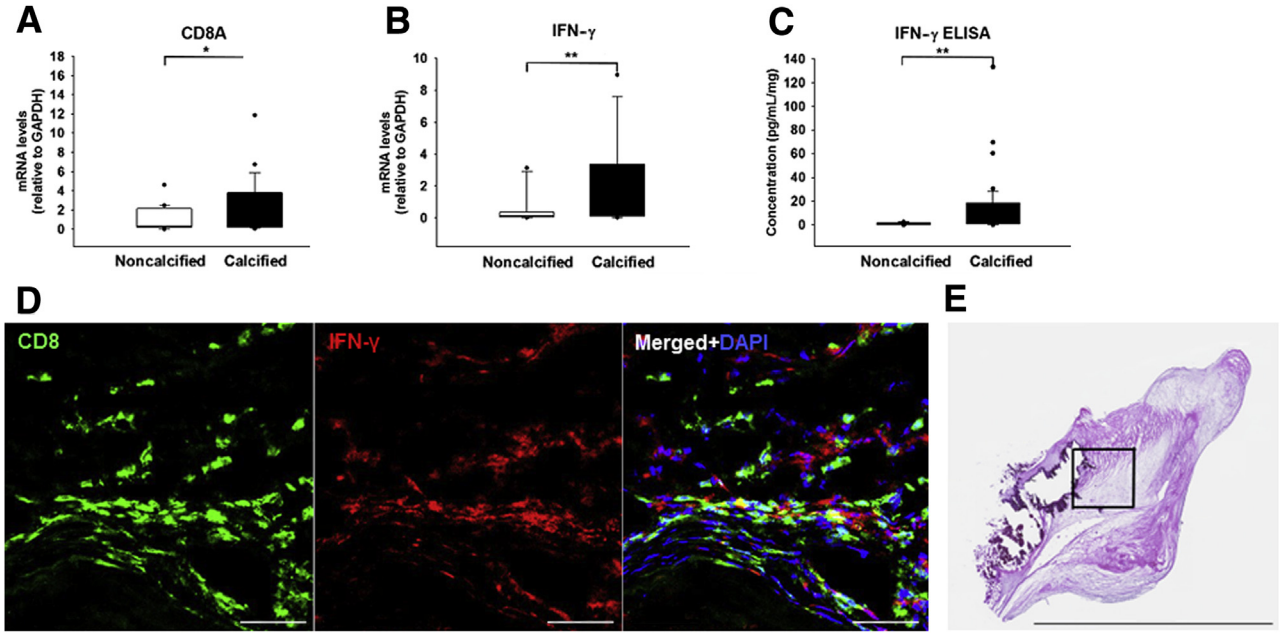

Figure 1 Calcified aortic valve cusps contain $CD8^+$ T cells and interferon (IFN)-γ. **A** and **B:** Relative gene expression (normalized to noncalcified areas of stenotic valves) of CD8A (**A**) and IFN-γ (**B**). **C:** IFN-γ enzyme-linked immunosorbent assay (ELISA). **D:** Double immunofluorescence staining indicating colocalization of $CD8^+$ T cells (green) and IFN-γ (red). The merged image shows colocalization and counterstaining with DAPI for visualization of the nuclei. **E:** Representative section of a calcified leaflet (transverse cryosection with a thickness on 6 μm), stained with hematoxylin and eosin to correlate histopathologic changes. The **boxed area** indicates an area adjacent to a calcified lesion, which is shown in **D**. $n = 116$ cusp portions from 52 valve donors (**A**–**C**); $n = 5$ (**D** and **E**). $^*P < 0.05$, $^{**}P < 0.01$. Scale bars: 50 μm (**D**); 5.632 mm (**E**). GAPDH, glyceraldehyde-3-phosphate dehydrogenase.

Supplemental Figure S1, A and B), as affirmed by the protein pattern (IFN-γ protein: 13.1- ± 3.6-fold, $P = 0.009$) (Figure 1C). In addition, calcified valve regions showed accumulation of $CD8^+$ T cells around calcified regions (Supplemental Figure S1, C–G). Double immunofluorescence staining demonstrated CD8–IFN-γ colocalization (Figure 1D) in calcified CAVD leaflets (Figure 1E). These observations suggest that infiltrating $CD8^+$ T cells accumulated in calcified regions in an activated state. In addition, in comparison with the noncalcified regions, calcified portions showed increased expression of cytotoxicity markers, such as Perforin 1 (4.3- ± 0.8-fold mRNA; $P = 0.003$) and GZMB (6.1- ± 1.8-fold mRNA; $P = 0.003$) (Figure 2, A–D, and Supplemental Figure S1, H and I), two signature proteins with cytolytic functions produced by activated cytotoxic $CD8^+$ T cells. Moreover, the heavily mineralized regions of the valve overwhelmingly expressed Hsp60, a phylogenetically highly conserved stress protein (3.8- ± 1.2-fold mRNA; $P = 0.013$) (Figure 2, E and F, and Supplemental Figure S1J), which suggested similarities to atherosclerosis and provided evidence for the presence of an antigen implicated in driving local adaptive immune responses.

Determination of the valvular expression profiles of the genes encoding the IFN-γ–induced T-cell–activating CXC chemokines, such as CXCL9, CXCL10, and CXCL11, followed. Although calcified parts revealed high levels of CXCL9 (3.9- ± 0.9-fold mRNA; $P = 0.015$) (Figure 2, G and H, and Supplemental Figure S1K), the transcripts of CXCL10 and CXCL11 remained unchanged (Supplemental Figure S2, A and B). Observations of the local expression of IFN-γ–producing $CD8^+$ T cells were extended by the findings on the significantly elevated levels of HLA-DR (Figure 2J and Supplemental Figure S1L) and its transcriptional co-activator, CIITA (2.9- ± 0.8-fold mRNA; $P = 0.028$) (Figure 2I), which the heavily calcified areas expressed abundantly, a characteristic associated with ongoing adaptive immune response. CCL2, another important chemokine also known as monocyte chemoattractant protein 1, actively participates in osteoclast differentiation. CCL2 showed only slightly elevated transcript levels in the calcified regions, yet these changes did not reach statistical significance (Supplemental Figure S2C). The osteoclast-associated genes showed differential expression patterns with significantly higher profiles of RANKL (6.4- ± 1.9-fold mRNA, $P = 0.009$; 4.5- ± 1.8-fold protein, $P = 0.046$) (Figure 3, A–C, and Supplemental Figure S1M), a cytokine favoring osteoclastogenesis, TRAP (8.3- ± 2.9-fold mRNA; $P = 0.007$) (Figure 3, D and E, and Supplemental Figure S1N), and OSCAR (3.5- ± 2.3-fold mRNA; $P = 0.017$) (Figure 3, F and G, and Supplemental Figure S1O), whereas that of Cathepsin K, a cysteine protease that resorbs the organic component of bone, which remains highly and selectively expressed by functional human osteoclasts, did not change (Figure 3H and Supplemental Figure S1P). The

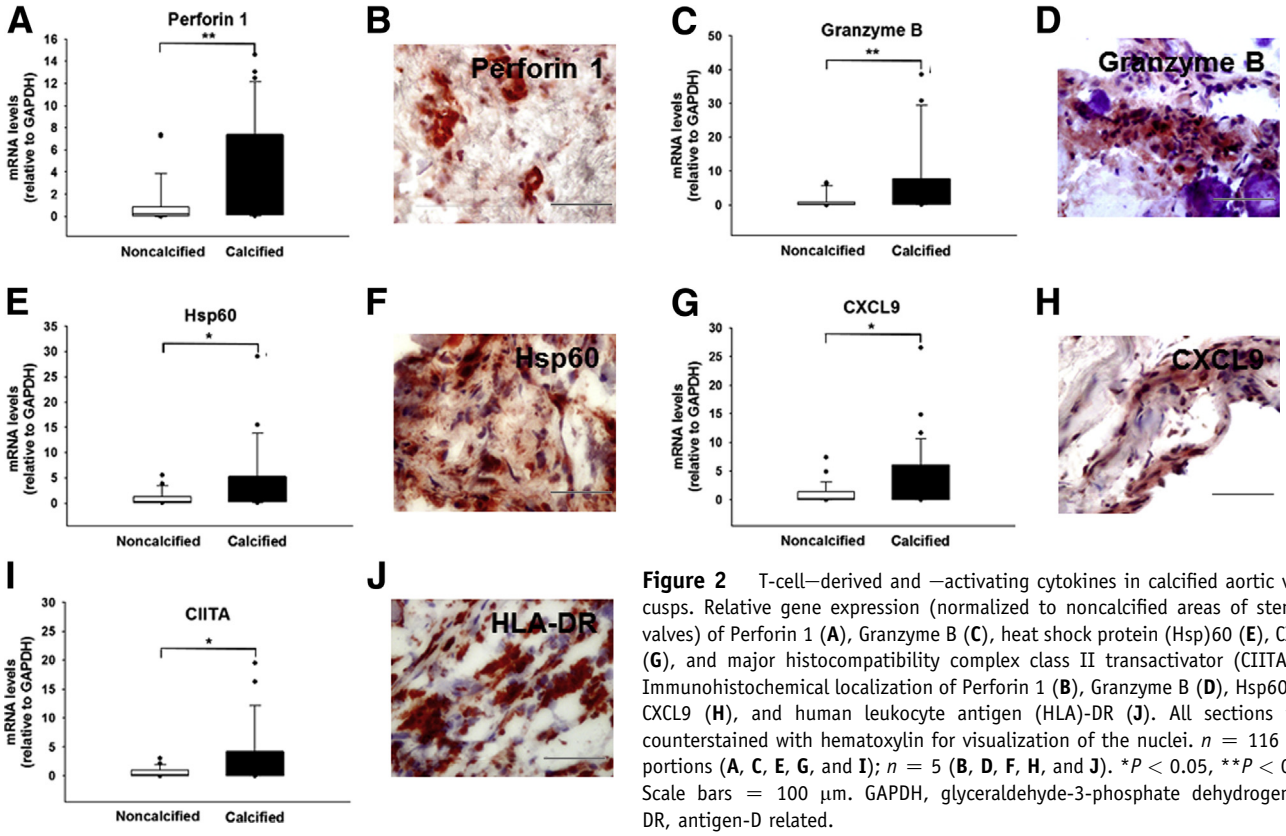

Figure 2 T-cell—derived and —activating cytokines in calcified aortic valve cusps. Relative gene expression (normalized to noncalcified areas of stenotic valves) of Perforin 1 (**A**), Granzyme B (**C**), heat shock protein (Hsp)60 (**E**), CXCL9 (**G**), and major histocompatibility complex class II transactivator (CIITA; **I**). Immunohistochemical localization of Perforin 1 (**B**), Granzyme B (**D**), Hsp60 (**F**), CXCL9 (**H**), and human leukocyte antigen (HLA)-DR (**J**). All sections were counterstained with hematoxylin for visualization of the nuclei. $n = 116$ cusp portions (**A**, **C**, **E**, **G**, and **I**); $n = 5$ (**B**, **D**, **F**, **H**, and **J**). $^{*}P < 0.05$, $^{**}P < 0.01$. Scale bars = 100 μm. GAPDH, glyceraldehyde-3-phosphate dehydrogenase. DR, antigen-D related.

combination of a low Cathepsin K, high TRAP and OSCAR expression suggested that ectopic valvular osteoclasts have impaired osteolytic activity, resulting in osteopetrotic features with subsequent high mineral density. Neither $CD4^+$ T cells nor mRNA for the regulatory T-cell—specific transcription factor forkhead box P3 changed significantly throughout the valve (Supplemental Figure S2, D and E). Although tissue IFN-γ was increased, the expression of its receptor IFNγR1 remained unaltered (Supplemental Figure S2F).

Activation of Valve T Cells Induces Reciprocal Changes of IFN-γ and RANKL Levels and Subsequently Promotes Valvular Calcium Load

The treatment of valve samples with a polyclonal T-cell activation cocktail containing PMA and ionomycin helped assess the effect of T cells on valve calcification. Parts of the specimens remained exposed to medium alone and served as controls. Stimulated portions had increased mRNA for IFN-γ (82.5- ± 27.5-fold; $P < 0.001$) (Figure 4A), GZMB (80.7- ± 50-fold; $P = 0.019$) (Figure 4B), unchanged levels of CD8A, consistent with *in vitro* $CD8^+$ T-cell activation and not proliferation (Figure 4C), and decreased transcripts of RANKL (0.005- ± 0.003-fold; $P = 0.003$) (Figure 4D). Protein measurements corresponded to these transcriptional changes, showing significant, robust, and prompt reciprocal changes in the concentrations (measured in the supernatant fluids) of IFN-γ (7.4- ± 2.5-fold day 1; 19.7- ± 9.3-fold day 2) (Figure 4E) and RANKL (0.1- ± 0.02-fold day 1; 0.3- ± 0.1-fold day 2) (Figure 4F). The net effect of *in vitro* $CD8^+$ T-cell activation resulted in significantly decreased expression levels of TRAP (0.011- ± 0.008-fold; $P = 0.015$) (Figure 4G) and Cathepsin K (0.0035- ± 0.002-fold; $P < 0.001$) (Figure 4H), a finding consistent with defective osteoclast function. Near infrared fluorescence imaging helped assess the functional consequences of the IFN-γ—mediated response. In the unstimulated control samples, no significant changes in calcium signal intensity occurred in the time-lapse images (Figure 5, A—E). In contrast, in T-cell—stimulated valve specimens, the calcium signal intensity increased gradually with a further significant rise on day 3 (1.6- ± 0.1-fold; $P < 0.001$), most likely due to immediate reciprocal changes of the local IFN-γ and RANKL expression on day 1 with a strong net inhibitory effect on osteoclastogenesis (Figure 5, F—J).

IFN-γ Treatment Leads to Formation of Morphologically and Functionally Defective Osteoclasts

The treatment of peripheral blood $CD14^+$ monocytes, isolated from healthy donors ($n = 6$), either with recombinant human IFN-γ or with an equivalent dose of endogenous IFN-γ, derived from conditioned medium of stimulated organoid cultures in the presence or absence of neutralizing

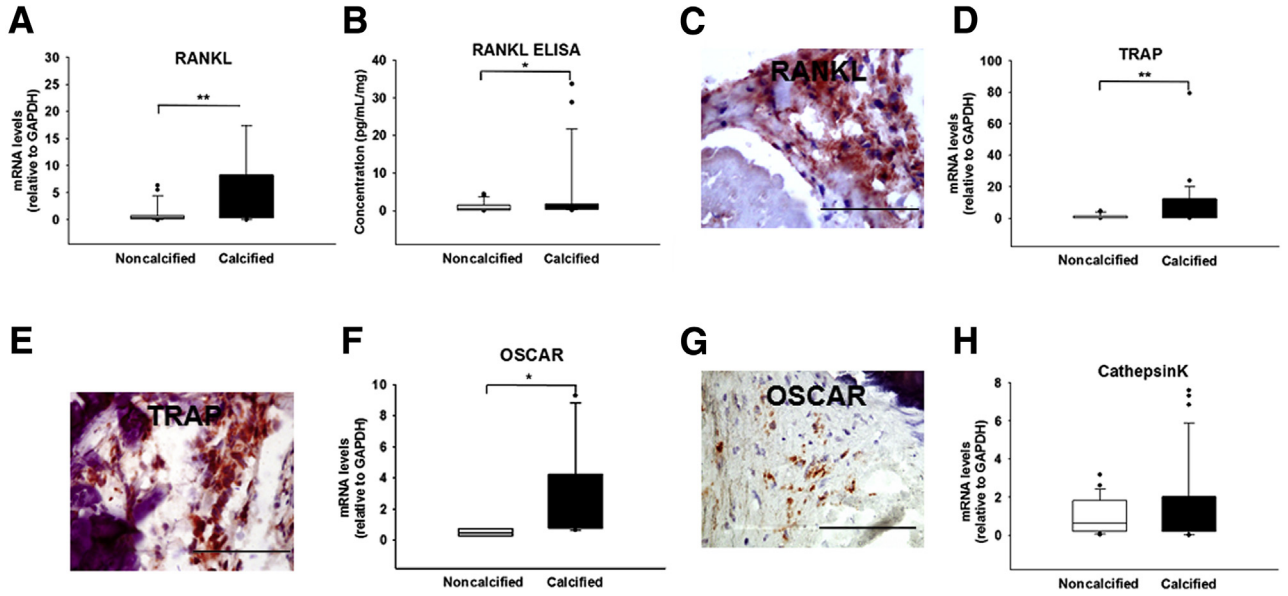

Figure 3 Osteoclast-related markers in calcified aortic valve cusps. **A**, **D**, **F**, and **H:** Relative gene expression (normalized to noncalcified areas of stenotic valves) of receptor activator of nuclear factor-κB ligand (RANKL; **A**), tartrate-resistant acid phosphatase (TRAP; **D**), osteoclast-associated receptor (OSCAR; **F**), and Cathepsin K (**H**). **B:** RANKL enzyme-linked immunosorbent assay (ELISA). **C**, **E**, and **G:** Immunohistochemistry for RANKL (**C**), TRAP (**E**), and OSCAR (**G**). All sections were counterstained with hematoxylin for visualization of the nuclei. $n = 116$ cusp portions (**A**, **D**, **F**, and **H**); $n = 75$ (**B**); $n = 5$ (**C**, **E**, and **G**). $^{*}P < 0.05$, $^{**}P < 0.01$. Scale bars = 100 μm. GAPDH, glyceraldehyde-3-phosphate dehydrogenase.

anti−IFN-γ antibody, helped evaluate the effects of IFN-γ on osteoclast function. Either source of IFN-γ consistently inhibited *in vitro* osteoclast activity, depicted by TRAP and morphologic changes, and evaluated by Rhodamine Phalloidin staining (Figure 6, A−C). The addition of neutralizing anti−IFN-γ antibody to IFN-γ−treated cultures abrogated the inhibitory effect of both forms of IFN-γ on osteoclast function and number ($P < 0.001$) (Figure 6, C and D) and the complete restoration of the observed cytoskeletal alterations. In parallel with these cellular morphologic alterations, IFN-γ triggered the inhibition of *in vitro* calcium resorption activity, whereas the addition of neutralizing anti−IFN-γ antibody restored it ($P < 0.001$) (Figure 6, C and E).

Treatment of osteoclast precursors with IFN-γ reduced expression levels of TRAP ($P = 0.02$), Cathepsin K

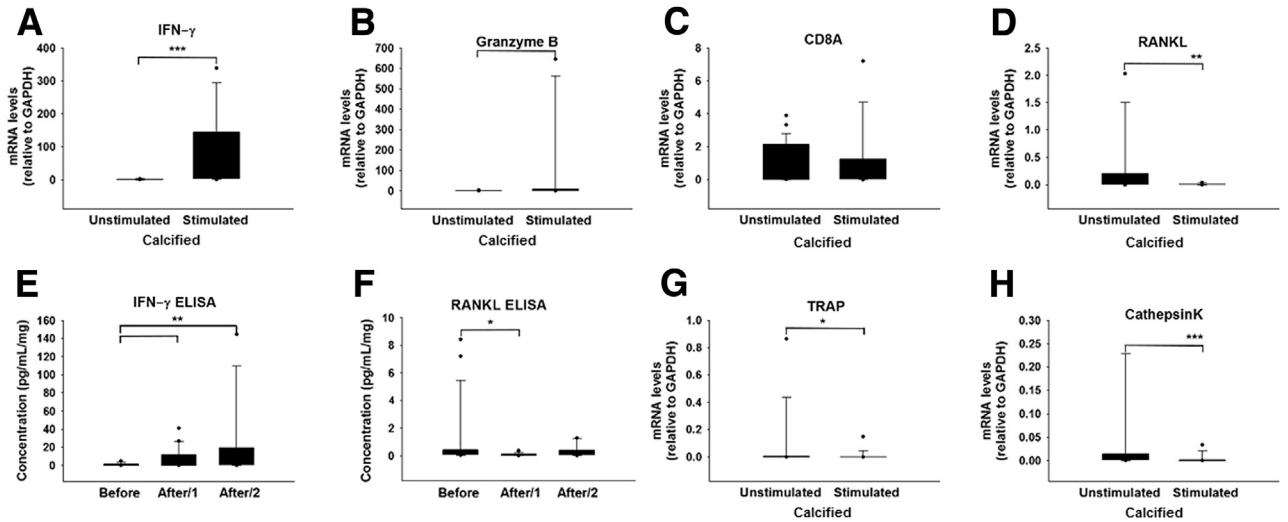

Figure 4 Interferon (IFN)-γ and osteoclast-related markers after T-cell activation in calcific aortic valve disease (CAVD) specimens. Relative gene expression (in stimulated calcified areas of stenotic valves, normalized to unstimulated calcified areas) of IFN-γ (**A**), Granzyme B (**B**), CD8A (**C**), receptor activator of nuclear factor-κB ligand (RANKL; **D**), tartrate-resistant acid phosphatase (TRAP; **G**), and Cathepsin K (**H**). Enzyme-linked immunosorbent assay (ELISA) for IFN-γ (**E**) and RANKL (**F**) in the conditioned medium before adding the cell activation cocktail (CAC), labeled as Before, and after 24 and 48 hours, indicated by After/1 and After/2, respectively. $n = 72$ cusp portions (**A**−**D** and **G**−**H**); $n = 63$ (**E**); $n = 20$ (**F**). $^{*}P < 0.05$, $^{**}P < 0.01$, and $^{***}P < 0.001$. GAPDH, glyceraldehyde-3-phosphate dehydrogenase.

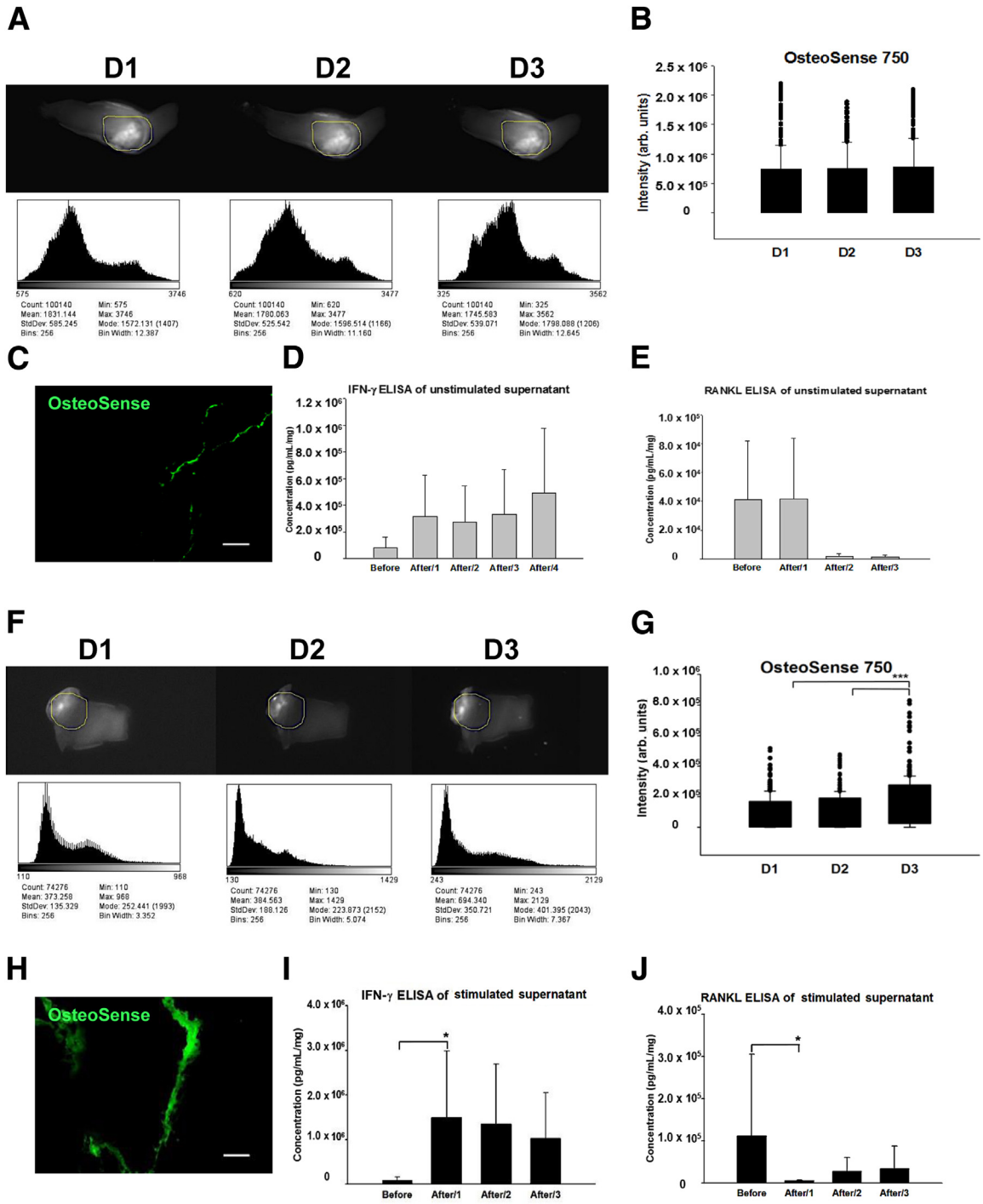

Figure 5 Molecular imaging monitoring the temporal and spatial changes in valvular calcium after T-cell activation in calcific aortic valve disease (CAVD) specimens. **A**–**E:** Data from unstimulated calcified areas of stenotic valves. **F**–**J:** Results from stimulated areas. signal intensity (SI) measurements were followed by quantification (ImageJ) within a region of interest (ROI; labeled with **yellow lines**, of which the position was aligned on all subsequent images). Each histogram corresponds to the distribution of SI and demonstrates the image characteristics for unstimulated (**A**) and stimulated (**F**) calcified parts. Quantification analyses show unchanged SI over time in **B** and significantly elevated SI in **G**. Near-infrared signal intensity (green) in unstimulated (**C**) and stimulated areas (**H**). Enzyme-linked immunosorbent assay (ELISA) for interferon (IFN)-γ and receptor activator of nuclear factor-κB ligand (RANKL), analyzed in unstimulated (**D** and **E**) and stimulated (**I** and **J**) supernatant fluids. $n = 4$ valve donors (**A**–**J**). $^{*}P < 0.05$, $^{***}P < 0.001$. Scale bars: 200 μm (**C** and **H**). Arb., arbitrary; D1, day 1 after activation; D2, day 2 after activation; D3, day 3 after activation.

($P = 0.007$), RANK ($P = 0.024$), a surface receptor on osteoclasts, and TRAF6 ($P = 0.004$), an adapter protein to RANK (Figure 6, F–I), whereas CD80 ($P = 0.012$) and CD86 ($P = 0.003$) levels rose in response to IFN-γ treatment (Figure 6, J and K). The addition of neutralizing anti–IFN-γ antibodies eliminated these effects (Figure 6).

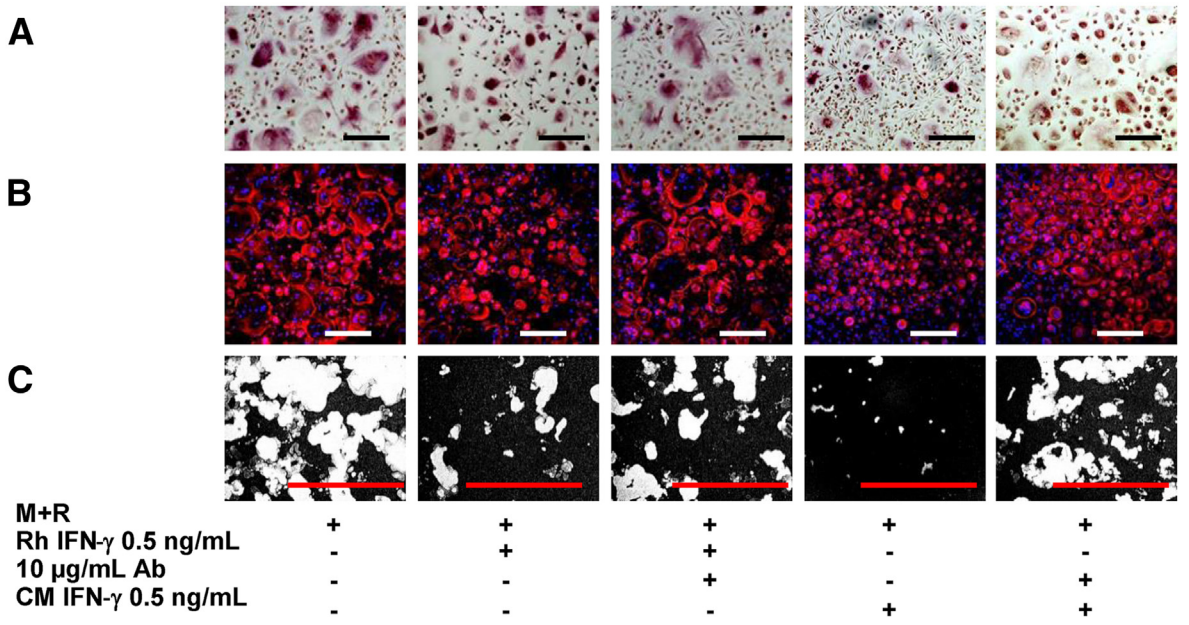
A
B
C
M+R
Rh IFN-γ 0.5 ng/mL
10 μg/mL Ab
CM IFN-γ 0.5 ng/mL

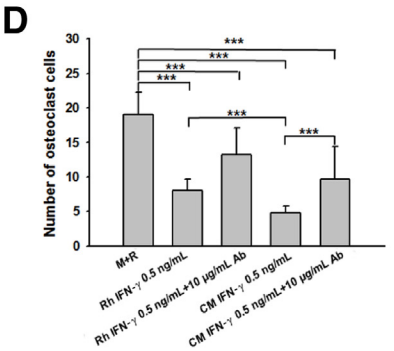
D
Number of osteoclast cells
M+R
Rh IFN-γ 0.5 ng/mL
Rh IFN-γ 0.5 ng/mL+10 μg/mL Ab
CM IFN-γ 0.5 ng/mL
CM IFN-γ 0.5 ng/mL+10 μg/mL Ab

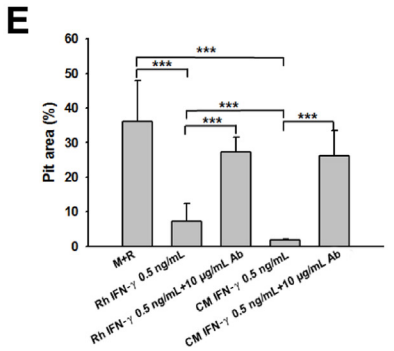
E
Pit area (%)
M+R
Rh IFN-γ 0.5 ng/mL
Rh IFN-γ 0.5 ng/mL+10 μg/mL Ab
CM IFN-γ 0.5 ng/mL
CM IFN-γ 0.5 ng/mL+10 μg/mL Ab

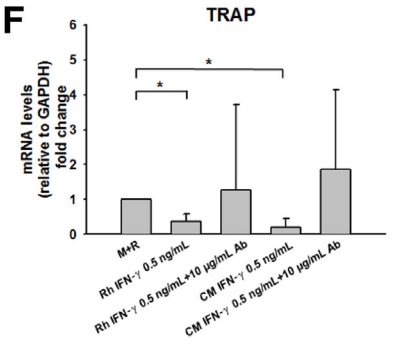
F
TRAP
mRNA levels (relative to GAPDH) fold change
M+R
Rh IFN-γ 0.5 ng/mL
Rh IFN-γ 0.5 ng/mL+10 μg/mL Ab
CM IFN-γ 0.5 ng/mL
CM IFN-γ 0.5 ng/mL+10 μg/mL Ab

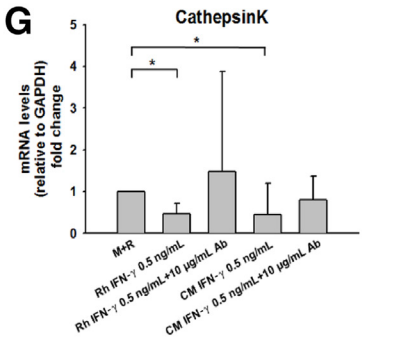
G
CathepsinK
mRNA levels (relative to GAPDH) fold change
M+R
Rh IFN-γ 0.5 ng/mL
Rh IFN-γ 0.5 ng/mL+10 μg/mL Ab
CM IFN-γ 0.5 ng/mL
CM IFN-γ 0.5 ng/mL+10 μg/mL Ab

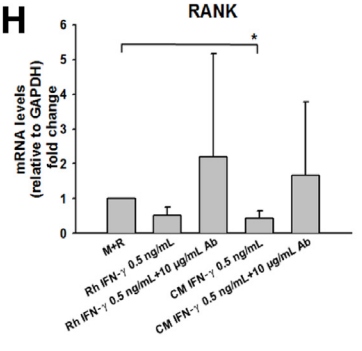
H
RANK
mRNA levels (relative to GAPDH) fold change
M+R
Rh IFN-γ 0.5 ng/mL
Rh IFN-γ 0.5 ng/mL+10 μg/mL Ab
CM IFN-γ 0.5 ng/mL
CM IFN-γ 0.5 ng/mL+10 μg/mL Ab

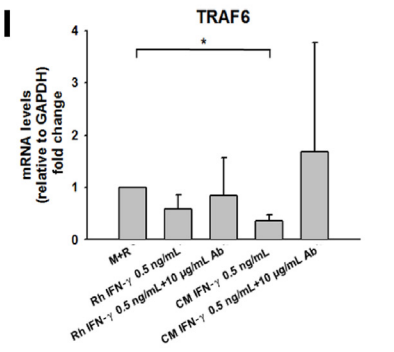
I
TRAF6
mRNA levels (relative to GAPDH) fold change
M+R
Rh IFN-γ 0.5 ng/mL
Rh IFN-γ 0.5 ng/mL+10 μg/mL Ab
CM IFN-γ 0.5 ng/mL
CM IFN-γ 0.5 ng/mL+10 μg/mL Ab

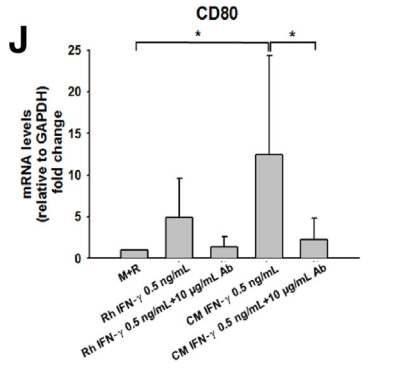
J
CD80
mRNA levels (relative to GAPDH) fold change
M+R
Rh IFN-γ 0.5 ng/mL
Rh IFN-γ 0.5 ng/mL+10 μg/mL Ab
CM IFN-γ 0.5 ng/mL
CM IFN-γ 0.5 ng/mL+10 μg/mL Ab

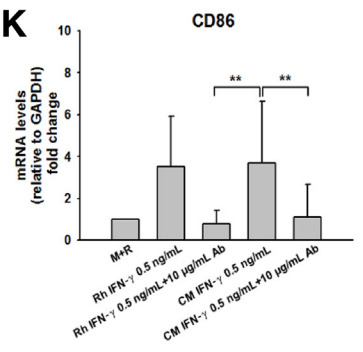
K
CD86
mRNA levels (relative to GAPDH) fold change
M+R
Rh IFN-γ 0.5 ng/mL
Rh IFN-γ 0.5 ng/mL+10 μg/mL Ab
CM IFN-γ 0.5 ng/mL
CM IFN-γ 0.5 ng/mL+10 μg/mL Ab

Discussion

These results support the concept that exaggerated IFN-γ release by activated valvular $CD8^+$ T cells impairs calcium resorption by valvular osteoclasts. The net effect of robust IFN-γ release from cytotoxic T cells activated *ex vivo* suppressed osteoclastogenesis with a subsequent increase in valvular calcium content, a condition that would favor progression of stenosis, an independent predictor of clinical outcome.[9] The *in vitro* experiments, which involved exposing osteoclast precursors to either recombinant human or endogenous IFN-γ from organoid culture–derived conditioned medium, showed significantly reduced numbers of $TRAP^+$ osteoclasts exhibiting decreased functionality, effects fully reversed by adding neutralizing anti–IFN-γ antibodies to the cultures. These findings support our hypothesis that adaptive immune response influences valvular calcium content through modulation of osteoclast functionality and thus facilitates CAVD progression.

This study used organoid cultures from surgically removed human stenotic aortic valves that contain resident cell populations, preserved in their original microenvironment. The presence of most of the local factors that may contribute to structural deterioration of the valve remains important. In addition, this approach simultaneously allows the close imitation and assessment of perturbations in the microenvironment at cellular and molecular levels, similar to the situation in the diseased valve, and may therefore serve as a useful tool to study CAVD. Because the isolation of mature osteoclasts from human vascular tissues presents a technical challenge, their functional state and ability to resorb bone remains largely unknown. *In vitro* studies are commonly performed using precursor cell populations isolated from peripheral blood. The extrapolation to *in vivo* conditions may prove misleading. Our results illustrate the utility of a combination of the *ex vivo*–maintained organoid cultures, suitable for functional assessment, along with complementary mechanistic cell culture experiments to evaluate pathologic processes at tissue and cellular levels. This approach permitted the quantification of osteoclast functionality in direct relation to the extent of valvular calcification.

The dominant feature of severe aortic valve stenosis is extensive dystrophic calcification (83%),[21] including microfractures at multiple sites, whereas lamellar bone formation (13%) marginally contributes to valvular mineralization.[21,30] In agreement with previous studies, heavily mineralized valve tissue harbors osteoclasts[21,22] with decreased although not completely silent osteolytic potential, probably due to low valvular expression levels of Cathepsin K, which is necessary for a normal resorptive capacity. These conditions resemble those described for a rare inherited bone disorder, called pycnodysostosis.[31] In valves, ectopic osteoclasts appear to function inefficiently; however, their increased numbers and protracted resorption time may counterbalance this impairment.

The aberrant and prolonged activation of IFN-γ–secreting $CD8^+$ T cells, which surround the calcified area,[8,12] support our concept. These $CD8^+$ T cells proliferate poorly but have strong effector activity and produce abundant inflammatory cytokines, including IFN-γ.[32]

The coexistence of abundantly expressed Hsp60,[8] one of the candidate autoantigens identified in atherosclerosis, *CXCL9*, an important T-cell–related gene,[32] and CIITA, its transcriptional co-activator that augments class II MHC expression and consequently facilitates antigen presentation to T cells,[32] indicates ongoing immunomodulation in advanced stages of the disease. Calcified regions also exhibited high expression of RANKL, possibly produced by activated myofibroblasts and T cells,[23] yet the local overexpression of IFN-γ may counterbalance RANKL. Similar to observations in the bone field that not only regulatory T cells[33] but also terminally differentiated effector $CD8^+$ T cells have a net inhibitory effect on osteoclastogenesis,[24,34] the present study provides evidence for an overall suppressive effect of activated $CD8^+$ T cells residing in the valve on osteoclast functionality. Because of impaired osteoclast function, the valvular calcium content may gradually increase in parallel with reciprocal and prompt changes in concentrations of IFN-γ and RANKL, suggesting that progressive loss of osteoclast resorptive potential contributes to the accumulation of valvular calcium.

The present *in vitro* studies using osteoclast precursor cells provide further evidence that IFN-γ accounts for the osteoclast-modulating activity in CAVD tissue, because anti–IFN-γ antibodies fully neutralized the presumably IFN-γ–mediated effects (ie, restored the numbers of functional $TRAP^+$ osteoclasts and their resorptive potential). The downstream molecular mechanisms by which IFN-γ suppresses osteoclastogenesis may include rapid

Figure 6 Interferon (IFN)-γ impairs osteoclastogenesis. Human $CD14^+$ monocytes were cultured in the presence of Rh IFN-γ or endogenous IFN-γ from conditioned medium (CM) IFN-γ in equivalent concentration (0.5 ng/mL). Neutralizing anti–IFN-γ Ab was added when indicated (10 μg/mL). **A:** Tartrate-resistant acid phosphatase (TRAP) staining. **B:** Morphologic changes of osteoclasts using Rhodamine Phalloidin staining, nuclei were counterstained with DAPI. **C:** Resorption pits (white) on black-and-white binary images (images were converted by ImageJ) in each treatment group. Representative areas of the cultures are shown for each condition. **D:** Numbers of osteoclasts with more than three nuclei per cell were counted and plotted in each group. **E:** Quantification of resorption pit areas (white), assessed as a percentage of the whole area. **F–K:** Relative gene expression data for TRAP (**F**), Cathepsin K (**G**), RANK (**H**), TRAF6 (**I**), CD80 (**J**), and CD86 (**K**). X-fold changes were calculated relative to M+R-treated wells. $n = 6$ human monocyte donors (**A–K**). $^*P < 0.05$, $^{**}P < 0.01$, and $^{***}P < 0.001$. Scale bars: 200 μm (**A–C**). Ab, antibody; GAPDH, glyceraldehyde-3-phosphate dehydrogenase; M, macrophage colony-stimulating factor at 25 ng/mL; R, receptor activator of nuclear factor-κB ligand at 30 ng/mL; Rh, recombinant human; TRAF, tumor necrosis factor receptor-associated factor.

degradation of RANK and its adapter protein, TRAF6, in accord with previous reports,[35] while increasing the expression of co-stimulatory molecules (CD80/CD86) required for T-cell activation by monocytes.[32]

The present study allowed sampling of several osteoclast and $CD8^+$ T-cell–related mediators at the tissue level and their relation to the osteoclast functionality in the context of CAVD. Limitations of this study include the relatively small sample size predicated on the availability of the human specimens and assessment of tissues obtained from patients with end-stage CAVD. In addition, we focused on osteoclasts and their functional state and not on the role of osteoblasts in the calcification process, which is reported in previous publications.[5] Therefore, this study cannot resolve the balance between active bone formation as an effect of osteoblast activity versus the increased calcification burden due to decreased osteoclast activity. As a further limitation, a sex-specific variation could not be excluded, which was not assessed in the present study.

The results of the present study provide new insight into the pathologic mechanisms of valvular calcification by demonstrating that activated infiltrating $CD8^+$ T cells with a highly altered cytokine profile can change ectopic osteoclast functions and thus may lead to enhanced valvular calcium accumulation. Therapeutic agents that selectively silence pathologic T-cell activation/T-cell response or selectively block IFN-γ may increase the resorptive activity of valvular osteoclasts and might limit the progression of CAVD.

Acknowledgments

We thank Eugenia Shvartz for excellent technical assistance and Chelsea Swallom for editorial expertise.

Supplemental Data

Supplemental material for this article can be found at *http://dx.doi.org/10.1016/j.ajpath.2017.02.012*.

References

1. Yutzey KE, Demer LL, Body SC, Huggins GS, Towler DA, Giachelli CM, Hofmann-Bowman MA, Mortlock DP, Rogers MB, Sadeghi MM, Aikawa E: Calcific aortic valve disease: a consensus summary from the Alliance of Investigators on Calcific Aortic Valve Disease. Arterioscler Thromb Vasc Biol 2014, 34:2387–2393
2. Nkomo VT, Gardin JM, Skelton TN, Gottdiener JS, Scott CG, Enriquez-Sarano M: Burden of valvular heart diseases: a population-based study. Lancet 2006, 368:1005–1011
3. Stewart BF, Siscovick D, Lind BK, Gardin JM, Gottdiener JS, Smith VE, Kitzman DW, Otto CM: Clinical factors associated with calcific aortic valve disease. Cardiovascular Health Study. J Am Coll Cardiol 1997, 29:630–634
4. Teo KK, Corsi DJ, Tam JW, Dumesnil JG, Chan KL: Lipid lowering on progression of mild to moderate aortic stenosis: meta-analysis of the randomized placebo-controlled clinical trials on 2344 patients. Can J Cardiol 2011, 27:800–808
5. Aikawa E, Nahrendorf M, Sosnovik D, Lok VM, Jaffer FA, Aikawa M, Weissleder R: Multimodality molecular imaging identifies proteolytic and osteogenic activities in early aortic valve disease. Circulation 2007, 115:377–386
6. Otto CM, Kuusisto J, Reichenbach DD, Gown AM, O'Brien KD: Characterization of the early lesion of 'degenerative' valvular aortic stenosis. Histological and immunohistochemical studies. Circulation 1994, 90:844–853
7. Towler DA: Molecular and cellular aspects of calcific aortic valve disease. Circ Res 2013, 113:198–208
8. Mazzone A, Epistolato MC, De Caterina R, Storti S, Vittorini S, Sbrana S, Gianetti J, Bevilacqua S, Glauber M, Biagini A, Tanganelli P: Neoangiogenesis, T-lymphocyte infiltration, and heat shock protein-60 are biological hallmarks of an immunomediated inflammatory process in end-stage calcified aortic valve stenosis. J Am Coll Cardiol 2004, 43:1670–1676
9. Rosenhek R, Binder T, Porenta G, Lang I, Christ G, Schemper M, Maurer G, Baumgartner H: Predictors of outcome in severe, asymptomatic aortic stenosis. N Engl J Med 2000, 343:611–617
10. Olsson M, Dalsgaard CJ, Haegerstrand A, Rosenqvist M, Ryden L, Nilsson J: Accumulation of T lymphocytes and expression of interleukin-2 receptors in nonrheumatic stenotic aortic valves. J Am Coll Cardiol 1994, 23:1162–1170
11. Wu HD, Maurer MS, Friedman RA, Marboe CC, Ruiz-Vazquez EM, Ramakrishnan R, Schwartz A, Tilson MD, Stewart AS, Winchester R: The lymphocytic infiltration in calcific aortic stenosis predominantly consists of clonally expanded T cells. J Immunol 2007, 178:5329–5339
12. Winchester R, Wiesendanger M, O'Brien W, Zhang HZ, Maurer MS, Gillam LD, Schwartz A, Marboe C, Stewart AS: Circulating activated and effector memory T cells are associated with calcification and clonal expansions in bicuspid and tricuspid valves of calcific aortic stenosis. J Immunol 2011, 187:1006–1014
13. Stemme S, Rymo L, Hansson GK: Polyclonal origin of T lymphocytes in human atherosclerotic plaques. Lab Invest 1991, 65:654–660
14. Swanson SJ, Rosenzweig A, Seidman JG, Libby P: Diversity of T-cell antigen receptor V beta gene utilization in advanced human atheroma. Arterioscler Thromb 1994, 14:1210–1214
15. Olsson M, Rosenqvist M, Nilsson J: Expression of HLA-DR antigen and smooth muscle cell differentiation markers by valvular fibroblasts in degenerative aortic stenosis. J Am Coll Cardiol 1994, 24:1664–1671
16. Andersson J, Libby P, Hansson GK: Adaptive immunity and atherosclerosis. Clin Immunol 2010, 134:33–46
17. Jonasson L, Holm J, Skalli O, Bondjers G, Hansson GK: Regional accumulations of T cells, macrophages, and smooth muscle cells in the human atherosclerotic plaque. Arteriosclerosis 1986, 6:131–138
18. Hansson GK, Jonasson L, Holm J, Claesson-Welsh L: Class II MHC antigen expression in the atherosclerotic plaque: smooth muscle cells express HLA-DR, HLA-DQ and the invariant gamma chain. Clin Exp Immunol 1986, 64:261–268
19. Roberts WK, Vasil A: Evidence for the identity of murine gamma interferon and macrophage activating factor. J Interferon Res 1982, 2:519–532
20. Olsson M, Thyberg J, Nilsson J: Presence of oxidized low density lipoprotein in nonrheumatic stenotic aortic valves. Arterioscler Thromb Vasc Biol 1999, 19:1218–1222
21. Mohler ER III, Gannon F, Reynolds C, Zimmerman R, Keane MG, Kaplan FS: Bone formation and inflammation in cardiac valves. Circulation 2001, 103:1522–1528
22. Nagy E, Eriksson P, Yousry M, Caidahl K, Ingelsson E, Hansson GK, Franco-Cereceda A, Back M: Valvular osteoclasts in calcification and aortic valve stenosis severity. Int J Cardiol 2013, 168:2264–2271
23. Kotake S, Udagawa N, Hakoda M, Mogi M, Yano K, Tsuda E, Takahashi K, Furuya T, Ishiyama S, Kim KJ, Saito S, Nishikawa T, Takahashi N, Togari A, Tomatsu T, Suda T, Kamatani N: Activated human T cells directly induce osteoclastogenesis from human monocytes: possible role of T cells in bone destruction in rheumatoid arthritis patients. Arthritis Rheum 2001, 44:1003–1012

24. Choi Y, Woo KM, Ko SH, Lee YJ, Park SJ, Kim HM, Kwon BS: Osteoclastogenesis is enhanced by activated B cells but suppressed by activated CD8(+) T cells. Eur J Immunol 2001, 31:2179−2188
25. Grcevic D, Lukic IK, Kovacic N, Ivcevic S, Katavic V, Marusic A: Activated T lymphocytes suppress osteoclastogenesis by diverting early monocyte/macrophage progenitor lineage commitment towards dendritic cell differentiation through down-regulation of receptor activator of nuclear factor-kappaB and c-Fos. Clin Exp Immunol 2006, 146:146−158
26. Cheng J, Liu J, Shi Z, Jules J, Xu D, Luo S, Wei S, Feng X: Molecular mechanisms of the biphasic effects of interferon-gamma on osteoclastogenesis. J Interferon Cytokine Res 2012, 32:34−45
27. Baumgartner H, Hung J, Bermejo J, Chambers JB, Evangelista A, Griffin BP, Iung B, Otto CM, Pellikka PA, Quinones M; American Society of Echocardiography; European Association of Echocardiography: Echocardiographic assessment of valve stenosis: EAE/ASE recommendations for clinical practice. Eur J Echocardiogr 2009, 10:1−25
28. Aikawa E, Nahrendorf M, Figueiredo JL, Swirski FK, Shtatland T, Kohler RH, Jaffer FA, Aikawa M, Weissleder R: Osteogenesis associates with inflammation in early-stage atherosclerosis evaluated by molecular imaging in vivo. Circulation 2007, 116:2841−2850
29. Lei Y, Iwashita M, Choi J, Aikawa M, Aikawa E: N-acetylglucosamine-1-phosphate transferase suppresses lysosomal hydrolases in dysfunctional osteoclasts: a potential mechanism for vascular calcification. J Cardiovasc Dev Dis 2015, 2:31−47
30. Torre M, Hwang DH, Padera RF, Mitchell RN, VanderLaan PA: Osseous and chondromatous metaplasia in calcific aortic valve stenosis. Cardiovasc Pathol 2016, 25:18−24
31. Saftig P, Hunziker E, Wehmeyer O, Jones S, Boyde A, Rommerskirch W, Moritz JD, Schu P, von Figura K: Impaired osteoclastic bone resorption leads to osteopetrosis in cathepsin-K-deficient mice. Proc Natl Acad Sci U S A 1998, 95:13453−13458
32. Libby P, Lichtman AH, Hansson GK: Immune effector mechanisms implicated in atherosclerosis: from mice to humans. Immunity 2013, 38:1092−1104
33. Buchwald ZS, Kiesel JR, DiPaolo R, Pagadala MS, Aurora R: Osteoclast activated FoxP3+ CD8+ T-cells suppress bone resorption in vitro. PLoS One 2012, 7:e38199
34. Buchwald ZS, Aurora R: Osteoclasts and CD8 T cells form a negative feedback loop that contributes to homeostasis of both the skeletal and immune systems. Clin Dev Immunol 2013, 2013:429373
35. Takayanagi H, Ogasawara K, Hida S, Chiba T, Murata S, Sato K, Takaoka A, Yokochi T, Oda H, Tanaka K, Nakamura K, Taniguchi T: T-cell-mediated regulation of osteoclastogenesis by signalling cross-talk between RANKL and IFN-gamma. Nature 2000, 408:600−605